

Simple Control for Complex Pandemics

Sarah C. Fay, Dalton J. Jones, Munther A. Dahleh, and A. E. Hosoi

Institute for Data Systems & Society

Massachusetts Institute of Technology

Cambridge, MA 02139, USA

(Dated: March 5, 2022)

arXiv:2012.08755v1 [q-bio.PE] 16 Dec 2020

Abstract

Amidst the current COVID-19 pandemic, quantifying the effect of strategies that mitigate the spread of infectious diseases is more important than ever. This article presents a compartmental model that addresses the role of random viral testing, follow-up contact tracing, and subsequent isolation of infectious individuals to stabilize the spread of a disease. We propose and examine two different models—a branching model and an individual-based model—both of which capture the heterogeneous nature of interactions that occur within a community. The branching model is used to derive analytical results for the trade-offs between the different mitigation strategies. The most important and perhaps surprising result from this analytical exercise is that a community’s stability to disease outbreaks is independent of its underlying network structure. This conclusion is then illustrated through simulation using both the branching model and the individual-based model.

I. INTRODUCTION

Communities around the world are fighting the COVID-19 pandemic. In the United States alone, more than 16 million cases and 300,000 deaths have been recorded in just 11 months [1]. In the absence of a vaccine, different mitigation strategies are required to reduce cases, fatalities, and outbreaks of the disease. The first measures many communities took were encouraging or mandating social distancing, i.e. reducing the number of interactions between members of a community, particularly interactions where transmission of the disease is likely [2–4]. These measures have been largely successful in slowing the rate at which the disease is spreading.

However, social distancing also prevents healthy people from interacting with each other, which has left many feeling isolated [5–7] and has hindered global economic activity [8, 9]. If we could successfully identify infectious individuals and isolate them before they spread the virus, people without the disease could safely be allowed to resume more normal levels of interaction. One way to detect infectious individuals is to check for symptoms. However, many cases of COVID-19 are asymptomatic [10, 11]; hence a different detection method is required, e.g. viral testing. This article analytically examines the effect of randomly testing the population for the disease with follow-up contact tracing and quantifies the trade-offs between social distancing and these detection methods.

As in most epidemiological studies, quantifying the effect of mitigation strategies hinges on creating a model of the disease dynamics. In this study, the number of infectious individuals is modeled as a stochastic branching process, a common model for disease behavior [12–14]. Because both the spread of the disease and eventual contact tracing depend on the network of interactions in a community [15–17], this network was included in our analysis through the number of contacts (i.e. interactions) belonging to each person (i) in the community, which is modeled as a random variable (X_i) whose distribution is unknown.

Using this approach, the mean and variance of the number of infectious individuals at a given time can be determined analytically. If both the mean and variance of the number of infectious individuals decay to zero, the dynamics are considered stable (because this condition ensures an initial outbreak will shrink to zero rather than grow uncontrollably). For this stochastic branching process, the stability condition is captured by a single effective reproduction number, which contains information about the network structure only through the mean number of contacts from the distribution X (and not through any higher moments). While this effective reproduction number is the same as would be found using an equivalent deterministic model that assumed homogeneous mixing in the population [18–20], this conclusion was derived using a heterogeneous interaction model implying that heterogeneity in social contacts does not impact the amount of testing required to stabilize the population.

Finally, while *stability* depends on the network only through its mean connectivity, using the model to predict the *size* of an outbreak would, in fact, require further knowledge of the underlying network structure, which has been examined in other studies [21–23]. The stability analysis detailed in this paper provides insight about the impact of different viral testing policies. These findings constitute the underlying engine in *whentotest.org* [24], a modeling tool that enables exploration of different mitigation strategies and the impact of those strategies on the spread of COVID-19. This website is currently being used by schools, businesses, and state policy-makers to help inform rational design of testing policies.

While this work was inspired by the COVID-19 pandemic, the results apply to any disease with similar characteristics, i.e. diseases where the susceptible population is large (no vaccine) and the spread is largely asymptomatic. The results of this study—in particular, the expression for the trade-offs between social distancing, testing, and contact tracing—do not depend on the specific disease parameters of COVID-19. Values of such parameters were used to illustrate the results, but the fundamental trade-offs apply to any disease with

similar attributes.

II. METHODS

A. Modeling foundation

In this article, we apply the principles established by Kermack and McKendrick [18] to model the spread of COVID-19 and similar diseases. Kermack and McKendrick’s model relies on partitioning the population into different categories based on disease status and applying a fundamental conservation law; while individuals may move among the partitions in the population (susceptible, infectious, recovered), the total number of people remains fixed. Mathematically, this means that the rate of change of the size of a particular partition is determined only by the net flow of individuals into or out of that group. Therefore, when we define stable dynamics as the case where the number of infectious individuals is shrinking, we could equivalently define it as the case where the flow of people out of this group is larger than the flow in.

Many extensions of the SIR model include additional classifications of individuals: some include an isolated/quarantined group [25], some include an exposed/latent group [20, 26], and still others include groups based on different population heterogeneities, e.g. age [27]. The choice of partitions relies on the particular disease of interest as well as the research questions driving the model. In our models, we partition the population into four groups: susceptible, infectious, isolated, and recovered. Because the aim of the study is to understand how testing and contact tracing (which lead to isolation) affect the spread of the disease, it is essential to include an isolated class. An exposed/latent group, which separates presymptomatic from symptomatic individuals, is not considered in this study due to the high number of COVID-19 cases that never become symptomatic [10, 11]. Additionally, by ignoring the development of symptoms, we will effectively *overestimate* the number of total infections, leading to more conservative stability bounds. Finally, this study assumes a homogeneous population (interacting in a heterogeneous way) for simplicity, but our model could easily be extended to differentiate between different groups (e.g. by age).

The choice of partitions and the flows between each group are depicted in Fig. 1. As noted above, stable disease dynamics are those for which the infectious class (shown in

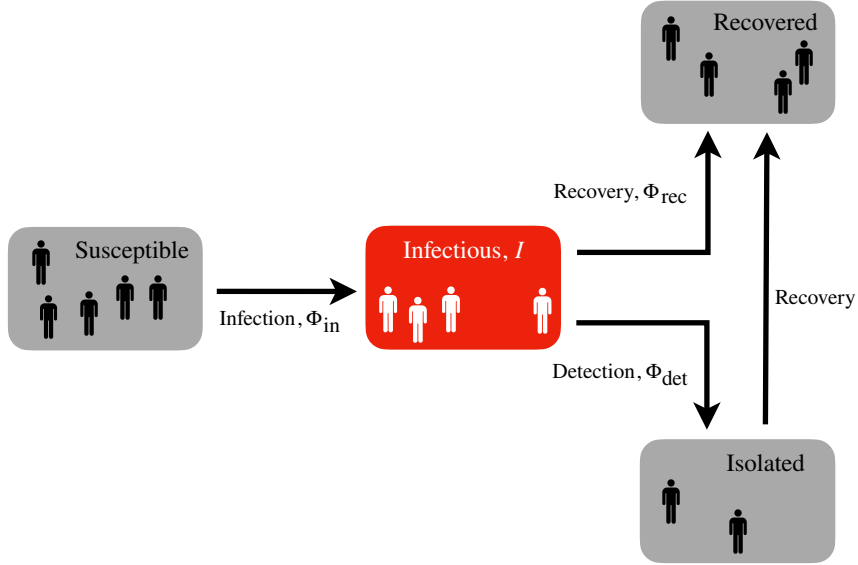


FIG. 1. Compartmental model for COVID-19 and similar diseases. Individuals join the infectious class (shown in red) by contracting the disease (at a rate Φ_{in}) and leave by recovering (Φ_{rec}) or by being detected and subsequently isolated (Φ_{det}).

red) is shrinking in size. The essential behavior of a disease, therefore, can be explored by modeling and tracking the the flow of individuals into and out of this group. In this model the rate of the flow (people per unit time) into the infectious class of individuals is denoted as Φ_{in} . The flow out of the infectious class is driven by two mechanisms. The first mechanism of out-flow is recovery. Individuals who recover from the disease are no longer able to infect others and therefore are no longer in the infectious group. The flow rate associated with recovery is denoted as Φ_{rec} . The other mechanism for out-flow is detection. If infectious individuals are detected, they can be isolated from the rest of the population. In this case, they no longer interact with susceptible members of the population and thus cannot infect others. The flow rate due to detection is denoted as Φ_{det} .

We can now write a conservation equation for the infectious group:

$$I_{t+1} - I_t = \Phi_{\text{in}} - \Phi_{\text{rec}} - \Phi_{\text{det}}. \quad (1)$$

This equation states that the change in our quantity of interest (the number of infectious people in the population), I , from one point in time (t) to the next ($t + 1$) must equal the

net flow of people into/out of the control volume during that unit of time.

This conservation equation lies at the heart of the analysis presented in this paper; it highlights the three levers that we can operate to reduce the spread of the disease and achieve controlled, stable dynamics. Our first lever is reducing the rate of infection (i.e. reducing Φ_{in}), which could be achieved by reducing the likelihood of transmission of the disease (e.g. by increasing social distancing or wearing face coverings). The second lever is to increase the rate of recovery. This lever is not easy to operate and is largely dictated by biological constraints and available medical treatments. The final lever, increasing detection, is the focus of this work. We examine how improved detection techniques—particularly the application of random viral testing, contact tracing, and subsequent isolation of infectious individuals—impact the disease dynamics.

In order to use the conservation law of Eq. 1, we must define each of the flows into and out of this group; namely, we choose constitutive relationships. Unlike the conservation law, these flows may depend on the details of the chosen model. In developing these relationships, we choose to extend on Kermack and McKendrick’s model in two other ways; first, we consider the behavior to be discrete, both in the number of individuals (no fractional people) and in time (information comes daily not continuously), and second we consider the processes of infection, detection, and recovery to occur stochastically. These two extensions are common in the literature [12, 13, 28] and more accurately describe observed disease behavior.

As one of the objectives of this study is to quantify the effect of contact tracing on mitigating the spread of a disease, the contacts/interactions between individuals in the population must be included in the model. This article presents two different ways to account for these interactions, a branching model [12, 13, 28] and an individual-based model (IBM) [15–17, 21]. These two models differ only in the way contacts between members of the population are represented and tracked. The first model, a branching model, does not track specific individuals in the population, only the total number of infectious people. The second model, an individual-based model, tracks the status of each member of the population at every point in time. While the individual-based model contains more information, the branching model can be more easily evaluated analytically allowing us to derive a simple quantitative estimate of how much random testing and contact tracing is required to stabilize the spread of a disease.

The details of the way the contacts are modeled in each case are included below, but first, we will establish their commonalities, namely their common parameters. We treat each of these parameters as constants in the stochastic process that we develop, but this analysis could easily be extended to the case where any or all of the parameters are instead also modeled as random variables. In both models, the rate of infection will depend on how many interactions an infectious person makes with other individuals at each time step, e.g. each day. The mean and variance in the number of interactions an infectious person makes will be denoted μ_x and σ_x^2 . If this interaction occurs between an infectious individual and a susceptible contact, the disease will be transmitted with probability ρ , commonly referred to as the transmissibility of the disease [19].

In defining recovery in both models, we assume that every infectious individual is equally likely to recover at a given time step. This likelihood is denoted $1/d$, where d is the average number of days spent infectious in the absence of detection methods. Using this model, we do not need to know or keep track of when each particular individual became sick, which is information that is typically not available for a real population. This memoryless behavior is consistent with Kermack and McKendrick’s original SIR model [18], though other choices may be more appropriate if more information is known about the distribution of the time until recovery or if more information is tracked about the individual members of the population.

These parameter definitions allow us to recover the basic reproduction number, \mathcal{R}_0 , of the disease

$$\mathcal{R}_0 = \rho\mu_x d. \tag{2}$$

This parameter, standard to modeling epidemiology, represents the number of “secondary cases one infectious individual will produce in a population consisting only of susceptible individuals” [19]. Given its frequent use in infectious diseases studies, the empirical value of this parameter may be more widely available and therefore more reliable than would be a measure of the transmissibility ρ . As Equation 2 connects the two through the mean number of contacts and the mean number of days until recovery, it can be used to rewrite our analysis in terms of this more familiar, accessible parameter.

The two final parameters of interest are related to the detection mechanisms, random testing and contact tracing, that this study aims to evaluate. Every member of the population, regardless of infection status, is equally likely to be chosen for random viral testing

on a given day. This likelihood is denoted as ν . Infectious individuals that are tested are assumed to be detected with 100% accuracy (though it is straightforward to later incorporate the sensitivity of the test) and immediately sent to isolation. The contacts of these detected individuals are then traced and isolated. The likelihood of successfully tracing a contact, meaning the contact was correctly identified and tracked down, is denoted as c . The constitutive relationships (i.e. the definitions of the flow rates) that allow for a fully formed model will depend both on these parameters and the choice of how interactions between individuals are modeled.

B. Branching model

In the branching model, the number of infectious individuals is considered but individual agents are not tracked. For instance, at time t , there are I_t infectious individuals whose identities are unknown. Similarly, without knowing who these individuals are we cannot know the identities of their contacts. However, we can model these interactions by assuming the number of contacts each infectious person has follows a distribution X with mean μ_x and variance σ_x^2 . Therefore, for each infectious individual i , we simulate their interactions by sampling from this distribution. In this study, we will assume that all of these contacts are with susceptible individuals. While considering contacts who are not susceptible (e.g. also infectious) is not difficult, by assuming all susceptible contacts, we effectively overestimate the number of infections that occur on each step, setting an upper bound on the stability criterion.

These susceptible individuals will then contract the disease and flow into the infectious population with probability ρ . The total number of new infections at time t can be written as

$$\Phi_{\text{in}} = \sum_{i=1}^{I_t} \sum_{j=1}^{X_i} Y_{ij}$$

where Y_{ij} is a Bernoulli random variable with parameter ρ and X_i is a different realization of the distribution of the number of contacts for each infectious person. Unlike in the SIR model, this infection term has no dependence on the size of the susceptible population [18]; by assuming that all contacts are susceptible, we have essentially assumed an infinite pool of susceptible people. To put this assumption in the context of the current pandemic, even

in the hardest hit regions like New York City, it is estimated that a little less than 20% of the population was infected [29], i.e. at least 80% of the population is still susceptible. This assumption does not affect the stability analysis which deals only with rates of change. However, if we wanted to use this model to forecast the number of people in a fixed population that were to get the disease, this model may be insufficient. One way to enable such prediction while still modeling interactions between individuals would be to use a model like the individual-based model discussed below.

The number of contacts of each infectious person also matters when considering detection through contact tracing. In order for one of these contacts (j) to be detected as infectious, two events must happen. First, the contact must actually be infectious at the time they are traced. At the previous time step, each contact had a likelihood ρ of being infected by person i . Using this as the likelihood that contact j is infectious at the current time step will *underestimate* the number of infectious contacts because person i may have been infecting their contacts for more than one day. Underestimating the number of infectious contacts and thus the number removed through contact tracing will lead to more robust stability bounds. In reality, it takes up to three days after initial exposure for the COVID-19 causing virus to become detectable through testing [30], however for simplicity we assume this can be done instantaneously. The second event that must occur is that this contact must be successfully traced. Each contact therefore has a probability $c\rho$ of being detected as infectious through contact tracing. Together, the number of infectious individuals removed from the population by detection via both random testing and contact tracing is

$$\Phi_{\text{det}} = \sum_{i=1}^{I_j} V_i \left(1 + \sum_{j=1}^{X_i} W_{ij} \right)$$

where V_i (random testing) and W_{ij} (tracing) are Bernoulli random variables with parameters ν and $c\rho$ respectively.

Unlike infection and detection, recovery does not depend on the number of contacts a person has. An infectious person has a likelihood of $1/d$ of recovering on a given day. However, to ensure we are not overestimating the flow out of the infectious population, we will only count those who recover *if* they are not chosen for testing on that day, which occurs with probability $1 - \nu$. The recovery flow rate is then

$$\Phi_{\text{rec}} = \sum_{i=1}^{I_t} Z_i (1 - V_i)$$

where Z_i is a Bernoulli random variable with parameter $1/d$.

Using the the constitutive relationships defined above and the conservation law of Eq. 1, the evolution of the number of infectious individuals (I) can be described as follows:

$$I_{t+1} = I_t + \sum_{i=1}^{I_t} \left[\left(\sum_{j=1}^{X_i} Y_{ij} \right) - Z_i (1 - V_i) - V_i \left(1 + \sum_{j=1}^{X_i} W_{ij} \right) \right]. \quad (3)$$

This stochastic difference equation is next examined analytically to uncover the range of parameters and particularly the amount of testing and contact tracing that stabilize the disease dynamics.

1. Stability analysis

Infectious disease dynamics are stable if the number of infectious individuals decrease on average. In the case of a stochastic model, there will always be a small probability that the number of infections could increase at each step. However, an application of Markov's inequality shows that if the expected number of infections $\mathbb{E}(I_t) \rightarrow 0$, then $\mathbb{P}(I_t > \epsilon) < \mathbb{E}(I_t)/\epsilon \rightarrow 0$. Hence, convergence of the mean dynamics guarantees the convergence of the stochastic process in probability. As such, when incorporating stochasticity, stability (controlled dynamics) will be defined for the mean dynamics: $\mathbb{E}[I_{t+1}] < \mathbb{E}[I_t]$ and must hold for all I_t . From Eq. 3 for the full stochastic process, the expectation of I_{t+1} can be written as:

$$\mathbb{E}[I_{t+1}] = \lambda \mathbb{E}[I_t] \quad (4)$$

where

$$\lambda = 1 + \rho \mu_x (1 - c\nu) - \nu - 1/d + \nu/d. \quad (5)$$

Stability ($\mathbb{E}[I_{t+1}] < \mathbb{E}[I_t]$) therefore requires that $\lambda < 1$, which contains no dependence on the variance in the distribution of the number of contacts σ_x^2 .

To put this in a familiar form, we can redefine λ in terms of an effective reproduction number \mathcal{R}_{eff} :

$$\lambda = 1 + r (\mathcal{R}_{\text{eff}} - 1) \quad (6)$$

where the effective reproduction number is given by

$$\mathcal{R}_{\text{eff}} = \mathcal{R}_0 \left(\frac{1 - c\nu}{1 + \nu(d-1)} \right) \quad (7)$$

and the parameter r is the likelihood of an infectious person being removed through either recovery or random testing given by

$$r = \nu + 1/d - \nu/d.$$

This new definition of λ (Eq. 6) allows us to view this as a classic control problem in which growth or decay is determined by the sign of $r(\mathcal{R}_{\text{eff}} - 1)$ and its magnitude determines the rate. A sufficient stability criterion for the mean dynamics is then $\mathcal{R}_{\text{eff}} < 1$. This result again highlights that stability depends only on the mean number of contacts each individual has and not on any other features of the underlying network of connections.

While the variance of the number of contacts σ_x^2 does not show up in the analysis of the expectation of I_{t+1} , it does arise when examining the variance, $\text{var}(I_{t+1})$. Computing this variance gives

$$\text{var}(I_{t+1}) = \gamma \mathbb{E}[I_t] + \lambda^2 \text{var}(I_t)$$

where λ is the same parameter defined in Eq. 5 and γ is derived as

$$\begin{aligned} \gamma &= \sigma_x^2 [\rho^2(1 + c^2\nu^2)] \\ &\quad + \mu_x [\rho(1 - \rho) + \rho c\nu(1 - \rho c\nu)] \\ &\quad + r(1 - r) \end{aligned}$$

where $r = \nu + (1 - \nu)/d$ and all of the parameters are defined as above.

We have that γ is obtained by noting that we calculate the conditional variance of Equation 3 as

$$\begin{aligned} \text{var} \left(I_t + \sum_{i=1}^{I_t} \left[\left(\sum_{j=1}^{X_i} Y_{ij} \right) - Z_i(1 - V_i) - V_i \left(1 + \sum_{j=1}^{X_i} W_{ij} \right) \right] \right) = \\ I_t \text{var} \left(\left(\sum_{j=1}^{X_i} Y_{ij} \right) - Z_i(1 - V_i) - V_i \left(1 + \sum_{j=1}^{X_i} W_{ij} \right) \right) \end{aligned}$$

so we need only calculate the variance of

$$\text{var} \left(\left(\sum_{j=1}^X Y_j \right) - Z(1 - V) - V - \sum_{j=1}^X W_j \right)$$

This random variable consists of three independent terms: new infections $\sum_{j=1}^X Y_j$, recoveries and tests $Z(1 - V) - V$, and contact tracing $\sum_{j=1}^{X_i} W_j$, where by construction W_j

is a Bernoulli random variable with parameter $c\rho\nu$. In this case, since these variables are independent we may sum their variances to attain our result. The variance of the recoveries and testing term is simply $r(1-r)$ where $r = \nu + (1-\nu)/d$. The other terms are slightly more involved, but we can invoke the law of total variance once again to see that by conditioning on the sampled degree we get

$$\begin{aligned} \text{var} \left(\sum_{j=1}^X Y_j \right) &= \text{var} \left[\mathbb{E} \left(\sum_{j=1}^X Y_j | X \right) \right] + \mathbb{E} \left(\text{var} \left[\sum_{j=1}^X Y_j | X \right] \right) \\ &= \text{var} (\rho X) + \mathbb{E} [\text{var} (\text{binom}(\rho, X))] \\ &= \text{var} (\rho X) + \mathbb{E} [\rho(1-\rho)X] \\ &= \sigma_x^2 \rho^2 + \rho(1-\rho)\mu_x \end{aligned}$$

since by conditioning on X we attain a binomial random variable with parameters ρ, X . The variance of the contact tracing term is obtained in the same way.

The disease dynamics can therefore be summarized by the two difference equations:

$$\begin{pmatrix} \mathbb{E} [I_{t+1}] \\ \text{var} (I_{t+1}) \end{pmatrix} = \begin{bmatrix} \lambda & 0 \\ \gamma & \lambda^2 \end{bmatrix} \begin{pmatrix} \mathbb{E} [I_t] \\ \text{var} (I_t) \end{pmatrix}. \quad (8)$$

A simple eigenvalue analysis shows that the system is stable to any initial values if both λ and λ^2 are less than 1. This means that stability in the mean is a sufficient condition for stability of the whole system.

C. Individual-based model (IBM)

As its name suggests, an individual-based model focuses on tracking the infection status of each member of the population. Rather than developing a network of contacts on-the-fly through branching, the network or graph is established at the outset. Every member of the population is a node of a graph, and every edge in the graph represents a contact between two individuals. Such a network is difficult to estimate (though techniques are improving [31]), but a random graph where connections make up a distribution inline with X_i can easily be created.

Once the underlying network of connections is established, each individual is assigned to one of the partitions of the model: susceptible, infectious, isolated, or recovered. At

each time step, the status of each individual is tracked. If a person is infectious they infect their susceptible neighbors (given through the network structure) with probability $\rho > 0$ at each time. If an individual is infectious at time t , they may recover at $t + 1$, an event with probability $1/d$. They may also become isolated if they are detected through random testing, an event with probability ν . If in fact they are detected in this way, each of their infectious neighbors has a probability c of also joining the isolated population. Isolated individuals will eventually recover and, on each step, have a likelihood of moving to the recovered population of $1/d$.

This process of tracking and evolving the statuses of each individual in the population constitutes the individual-based model. The flow of individuals and the size of the infectious population can be tracked through by a simple counting process. This model is straight-forward to simulate computationally, though much more information (e.g. the graph structure) must be tracked—and hence more memory is required—than when simulating the branching model. The individual-based model does not readily lend itself to theoretical analysis but is popular because it can accurately predict the size and progression of an outbreak over time. This lack of tractability is the reason we focus on deriving analytical results using the stochastic branching model [15–17]. This article compares the analytical results found using the branching model to the computational results using both the branching model and this individual-based model. Through these exercises, contrary to popular belief [15–17, 22], we find that stability depends only on the mean number of contacts people in the population have, and it does not depend on any other aspect of the network structure such as high centrality individuals.

III. RESULTS

A. Comparing mitigation strategies

The stability analysis performed on the branching model allows us to reduce the spread of a disease to a single parameter, the effective reproduction number \mathcal{R}_{eff} of Eq. 7. This parameter represents the expected number of secondary infections that will result from a single infectious individual under the given testing and contact tracing protocols and is a common disease descriptor in epidemiology [19]. If this number is less than one, the disease

is considered to be contained, as the number of cases (as well as this number’s variance) is expected to decrease; if it is greater than one, outbreaks will grow uncontrollably.

The relevant policy parameters contained in the expression for the effective reproduction number (see Eq. 7) are the fraction of the population chosen randomly to be tested each day, ν , and the percent of contacts that we expect to successfully trace, c . The parameters associated with the disease are the average number of days that a person spends being infectious after contracting the disease, d , and the basic reproduction number, \mathcal{R}_0 , which represents the number of secondary infections in a fully susceptible population where no detection methods are in place. The basic reproduction number is commonly measured from case counts and reported in disease literature [30, 32, 33]. Notice, if we consider the case where no testing or contact tracing is occurring, the expression simplifies to $\mathcal{R}_0 < 1$, which, by definition, represents stable dynamics for a disease in a fully susceptible, naive population [19].

The basic reproduction number also captures the amount of social distancing that is occurring in the community; it can be expressed as $\mathcal{R}_0 = \rho\mu_x d$ (Eq. 2) where μ_x is the mean number of people that a member of the community interacts with each day and ρ is the likelihood that such an interaction would lead to the transmission of the disease. Social distancing often consists of both reducing the number of contacts per day (decreasing μ_x) as well as changing the nature of these interactions, e.g. through wearing masks (decreasing ρ). In this analysis, the basic reproduction number therefore captures the social distancing policies and behaviors. In terms of the underlying network of the interactions in the community, the mean number of contacts, μ_x , is the mean connectivity of that network. The reproduction number does not depend on any other information about this underlying network structure, such as the presence or number of highly connected individuals. However, when determining the reproduction number empirically, having information about the underlying network can improve the accuracy of the measurement [31].

The stability criterion ($\mathcal{R}_{\text{eff}} < 1$) provides simple guidance on how much random testing and contact tracing are required to mitigate the spread of a disease. By rearranging this expression, the minimum amount of testing required to ensure stability to outbreaks is found to be

$$\nu_{\min} = \frac{\mathcal{R}_0 - 1}{c\mathcal{R}_0 + d - 1}. \quad (9)$$

This relationship can be used to compute the minimum required daily testing fraction for

TABLE I. Comparison between the levels of random testing needed to control the spread of different common diseases for two contact tracing scenarios. The rate of testing indicates the probability of an individual being tested on each day; i.e. 1 corresponds to daily testing for everyone ; 0.5 corresponds to testing half the population each day. The required level of testing decreases as contact tracing increases, as in the the fourth column where 50% of contacts are traced after a successful test. Note: estimates for COVID-19 are based on aggregate global data [30].

	\mathcal{R}_0	Days Infected	Testing only	Testing ($c = 0.5$)
COVID-19	4.5 [30]	14 [30]	0.27	0.23
Influenza	1.4 [34]	7 [34]	0.07	0.06
Measles	12.0 [32]	14 [32]	0.85	0.58
Mumps	4.28 [33]	12[33]	0.30	0.25
Polio	5.0 [35]	7 [35]	0.67	0.47
SARS	1.08 [36]	14 [36]	0.006	0.004
Smallpox	5.0 [37]	21 [37]	0.20	0.18

various diseases. The results for some specific diseases (including COVID-19) are shown in Table I. The table contains both the required testing fraction for the case of no contact tracing ($c = 0$) and the case where 50% of contacts are successfully traced ($c = 0.5$). The specific parameters selected are mean values taken from the literature for spread under normal conditions, i.e. no social distancing. Because some of these diseases can be and are managed in ways other than testing (e.g. through vaccination or symptom identification), the provided testing fractions are not always used in practice.

Regardless of the specific disease and its associated parameters, the expression for the minimum required testing fraction (Eq. 9) shows the trade-offs between social distancing, testing, and contact tracing. First, we see that no testing is required ($\nu_{\min} = 0$) if and only if $\mathcal{R}_0 \leq 1$; the disease is already considered to be under control. Next, to illustrate the relationship between testing and social distancing, we consider the case where no contact tracing is done: $c = 0$. The minimum required testing fraction simplifies to

$$\nu_{\min,c=0} = \frac{\mathcal{R}_0 - 1}{d - 1}.$$

This relationship shows that decreasing social distancing (i.e. increasing the amount of

daily interactions: μ_x in \mathcal{R}_0) requires that more testing be done to control the spread of the disease. Put another way, if more testing is available, less social distancing is required.

In actuality, the amount of daily testing is limited by a community's resources, e.g. available tests, processing facilities, labor, etc. In the case where these resources are limited, communities can still safely increase the frequency of normal interactions (\mathcal{R}_0) if they can increase contact tracing abilities (c). Contact tracing may also be a limited resource in terms of the labor required and the immediacy with which it is useful.

The trade-offs expressed analytically in Eq. 9 are visualized in Fig. 2 for a disease with a mean infectious period of 14 days, as is the case for COVID-19 [30]. As the amount of testing increases, the allowable \mathcal{R}_0 increases as well, and these gains in social interactions are greatest when more contact tracing is done. Also shown in Fig. 2 are the mean measured reproduction numbers in three different scenarios: Wuhan communities [38], a global average [30], and aboard the Diamond Princess cruise ship [39]. While the case data used to arrive at these values largely occurred before robust, large-scale testing methods were established, examining these scenarios allows us to predict how much testing and contact tracing would be required to support communities in the future based on the expected level of social interaction occurring. While more social interaction will require more testing and contact tracing, stable dynamics can still be achieved in most scenarios if the resources are available.

This analysis quantifies the effects of social distancing, testing, and contact tracing in mitigating the spread of an infectious disease. Which particular strategies are employed will depend on the specific community and its resources. Using the effective reproduction number as a constraint, the analysis above can be extended to include the economic costs of these mitigation strategies. By associating the cost of testing, contact tracing, and reduced interaction with the relevant parameters, we can find the minimum cost solution that still achieves stable dynamics.

B. Simulation

To demonstrate the efficacy of the analytic expressions above and to illustrate the trade-offs between social distancing, testing, and contact tracing, simulations of the underlying stochastic SIQR model were run. The simulations also allowed for testing of different models

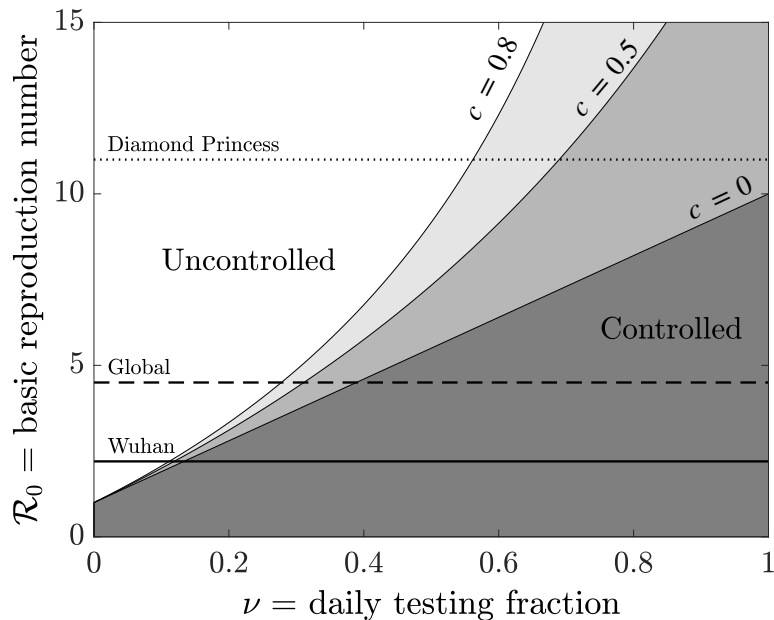


FIG. 2. Trade-offs between social distancing, testing and contact tracing. The stability boundary between scenarios of controlled and uncontrolled disease behavior are shown. Horizontal lines represent mean reproduction numbers for COVID-19 in early Wuhan studies [38] (solid), global aggregate values [30] (dashed), and on the Diamond Princess cruise ship [39] where little social distancing was possible (dotted).

for the underlying network of interactions in the community. Results confirm the analytical expression which states that only the mean connectivity of the network (i.e. the mean number of daily interactions averaged across the population) affects whether or not the disease can be contained.

Two different classifications of community network models were tested: a branching model [12, 28] and an individual-based model (IBM) [15–17]. The individual-based model requires generating a graph that represents the community structure before simulating the spread of the disease, whereas the branching model generates the graph on the fly. In both cases, the distribution of edges in the graph, i.e. the number of interactions a person has, can take any form. Two specific distributions, a binomial distribution and a uniform distribution, were tested.

Fig. 3 shows the results of running these simulation for a small outbreak (10 infected

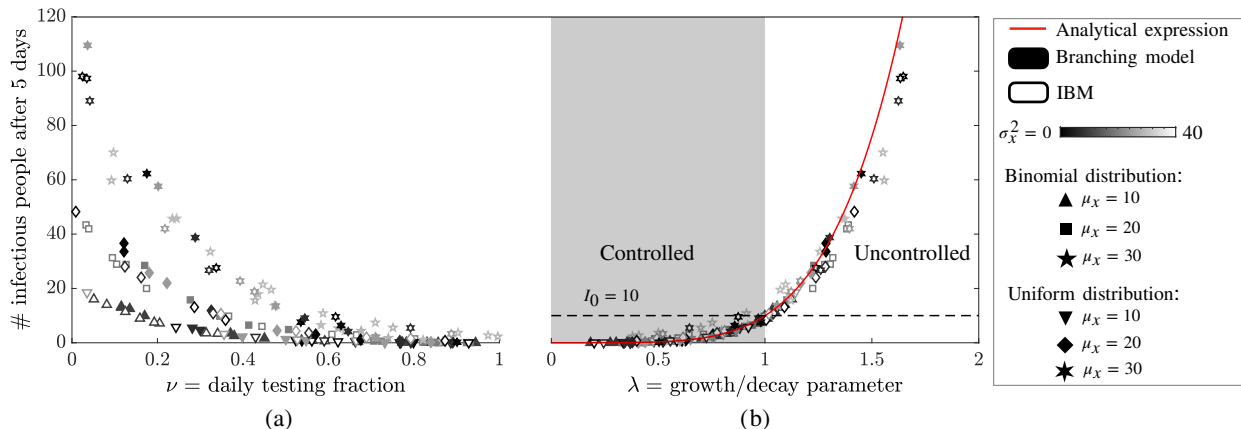


FIG. 3. Number of infectious individuals at $t = 5$ for $I_0 = 10$ (dashed line) as a function of (a) the daily testing fraction and (b) the parameter λ , for various models of interactions in the population. The collapse in λ shown in (b) indicates that stability is independent of the variance and type of distribution of interactions. The shaded region represents where we expect to see stable dynamics, i.e. where the number of infectious individuals decreased from I_0 . Each point represents the mean of 100 trials with the same parameters.

individuals) for a span of 5 days (for a fixed disease transmissibility ρ , mean infectious period d , and fraction of successfully traced contacts c). Each point represents the mean number of infectious individuals on day 5 over 100 trials. Fig. 3(a) shows that more random testing leads to there being fewer infectious people after 5 days and a more controlled outbreak. However, the amount of testing needed to see decreasing case numbers depends on the average number of daily interactions μ_x ; as expected, underlying graphs with higher connectivity require more rigorous testing.

Analysis of the SIQR model shows that the expected growth/decay in the number of infectious individuals (I) in a day (from t to $t + 1$) is governed by Eq. 4 ($\mathbb{E}[I_{t+1}] = \lambda \mathbb{E}[I_t]$). Because of the linear time-invariant nature of Eq. 4, the number of infectious individuals on any future day will depend only on the size of the initial outbreak and on the parameter λ (defined in Eq. 5).

This growth/decay rate depends only on the mean number of daily interactions a person has (μ_x) and not on the variance or form of the associated distribution. Fig. 3(b) corroborates this result as it shows a collapse in the simulation data to the analytical result for all

of the different models and distributions of the underlying graph.

IV. DISCUSSION

While this work was originally inspired by the necessity to use testing and other non pharmaceutical interventions to control the spread of COVID-19, the results derived depend on neither the particular characteristics of this disease nor the structure of the network along which it is transmitted. This allows one to generalize using the relationship between the effective reproduction number \mathcal{R}_{eff} and the amount of testing and contact tracing. In particular, given some estimate of the parameters of a disease's proliferation, the stability analysis performed in this paper gives guidelines on the amount of testing and contact tracing needed to stop outbreaks of a disease.

In particular, as seen in Table I, without any other policy interventions, in order to stop a disease like measles from spreading in a fully susceptible population, 85% of the population would need to be tested *daily*. For this reason, vaccinating for measles in order to reduce the number of susceptible individuals is essential. The stability criteria can be used in any situation in which relevant parameters (such as \mathcal{R}_0) can be estimated, but provides the most practical guidance in cases where there is a large susceptible population and a large proportion of asymptomatic cases. Finally, it is important to emphasize that the stability criteria *does not* depend on the variance of the underlying network of the community, only its average degree; highly connected individuals only impact the dynamics through their contribution to the mean. This simplifies the analysis of the spread of an epidemic as it proves to be independent of network structure.

Another important subtlety arises as, for example, the \mathcal{R}_0 parameter is estimated over time. As the disease progresses and policies are put in place to slow the spread, this estimation will change. In particular, if testing is put into place, we can think of this as reducing the number of connections in the original graph and hence, the expression obtained in this case for the amount of testing needed to stabilize the dynamics represents the additional amount of testing needed. Thus, for the purposes of allocating testing and contact tracing resources, it is not necessary to understand the particulars of the disease, a relatively coarse measurement, possibly obscured by the inclusion of previous control methods still allows one to predict the additional resources necessary to mitigate disease spread.

A. Policy implications

One of the most important implications of this work is that with knowledge of only a few disease parameters, one can determine the amount of testing and contact tracing needed to prevent major outbreaks in a pandemic. In addition, the relationships derived in the stability criteria relate different amounts of testing and social distancing to the rate of the pandemic’s spread. Hence, we obtain an understanding of the trade-offs policymakers must make as social distancing is increased or decreased; in a sense, we get a “value of social connections” in terms of the additional amount of testing needed as social distancing is relaxed. These guidelines are particularly important for COVID-19 since, without a vaccine or treatment, the only reliable ways to control the spread of the disease are non-pharmaceutical (e.g. social distancing, testing, contact tracing).

The parameters that need to be estimated to compute the amount of testing needed to stabilize the disease dynamics can be estimated via local case counts. Additionally, if there is some uncertainty in the values of these parameters, policymakers can create robust control policies by allowing these parameters to take on “worst case” values. In the case of COVID-19, estimates for \mathcal{R}_0 reach 11 for highly confined situations like aboard a cruise ship [39]. To ensure stable dynamics in this case, 75% of the passengers would need to be tested daily.

It should also be pointed out that an implicit assumption underlying the development of the bounds for stability was that individuals do not ever become symptomatic and remove themselves from the population. This means that the bounds derived are indeed upper bounds on the required amount of testing and contact tracing necessary to achieve stability. Finally, if these results are combined with a dynamic estimation of parameters, one would obtain a feedback loop which would adjust to time varying effects (e.g. seasonality of social distancing) to recommend the required stabilizing levels of random testing.

This work has been applied in the development of a web application which can be found at *whentotest.org* [24], which is a tool that incorporates our stability analysis to recommend how much testing should be done in a population given certain characteristics. In particular, organizations such as schools or businesses input characteristics of their members and work environment (including mitigation strategies like mask wearing and contact tracing) and the web application will recommend a testing policy including a number and type of tests per

week. This tool is already being utilized by some colleges and even larger entities like the state of Connecticut and its effectiveness in the real world has been demonstrated by the success of the testing policy on college campuses like MIT.

B. Modeling implications

Our analysis showed that stability to outbreaks depends on the underlying network of the community only through its mean connectivity. This result allowed us to quantify trade-offs between different mitigation strategies on the spread of disease that apply to all communities, not just those whose interaction behaviors are roughly homogeneous. Our results imply that when only examining stability, a powerful tool for quantifying trade-offs between non-pharmaceutical interventions, higher complexity network models (those with more information about the underlying community structure than simply its mean degree) are unnecessary. However, if instead we wanted to use our epidemiological model to predict the size of an outbreak, models that contain more detailed network information are important.

ACKNOWLEDGMENTS

S.C.F. was partially supported by the adidas Future team. D.J.J was supported by C3.ai Digital Transformation Institute Agreement dated 5/22/2020.

-
- [1] CDC, *Coronavirus Disease 2019 (COVID-19): Cases and Deaths in the U.S.* (2020 (accessed December 15, 2020)).
 - [2] D. J. McGrail, J. Dai, K. M. McAndrews, and R. Kalluri, Enacting national social distancing policies corresponds with dramatic reduction in covid19 infection rates., *PLoS ONE* **15**, 1 (2020).
 - [3] T. P. B. Thu, P. N. H. Ngoc, N. M. Hai, and L. A. Tuan, Effect of the social distancing measures on the spread of covid-19 in 10 highly infected countries., *Science of the Total Environment* **742** (2020).

- [4] A. Teslya, T. M. Pham, N. G. Godijk, M. E. Kretzschmar, M. C. J. Bootsma, and G. Rozhnova, Impact of self-imposed prevention measures and short-term government-imposed social distancing on mitigating and delaying a covid-19 epidemic: A modelling study., *PLoS Medicine* **17**, 1 (2020).
- [5] R. Elran-Barak and M. Mozeikov, One month into the reinforcement of social distancing due to the covid-19 outbreak: Subjective health, health behaviors, and loneliness among people with chronic medical conditions., *International journal of environmental research and public health* **17** (2020).
- [6] J. G. Luiggi-Hernández and A. I. Rivera-Amador, Reconceptualizing social distancing: Teletherapy and social inequality during the covid-19 and loneliness pandemics., *Journal of Humanistic Psychology* **60**, 626 (2020).
- [7] K. Lewis, Covid-19: Preliminary data on the impact of social distancing on loneliness and mental health., *Journal of psychiatric practice* **26**, 400 (2020).
- [8] F. Milani, Covid-19 outbreak, social response, and early economic effects: a global var analysis of cross-country interdependencies., *Journal of population economics* , 1 (2020).
- [9] H. Simola and L. Solanko, Domestic and global economic effects of covid-19 containment measures: How does domestic and global economic effects of covid-19 containment measures: How does russia compare internationally?., *BOFIT Policy Brief* , 3 (2020).
- [10] D. He, S. Zhao, Q. Lin, Z. Zhuang, P. Cao, M. H. Wang, and L. Yang, The relative transmissibility of asymptomatic covid-19 infections among close contacts., *International Journal of Infectious Diseases* **94**, 145 (2020).
- [11] A. Kronbichler, D. Kresse, S. Yoon, K. H. Lee, M. Effenberger, and J. I. Shin, Asymptomatic patients as a source of covid-19 infections: A systematic review and meta-analysis., *International Journal of Infectious Diseases* **98**, 180 (2020).
- [12] M. Peak Corey, M. Childs Lauren, H. Grad Yonatan, and O. Buckee Caroline, Comparing non-pharmaceutical interventions for containing emerging epidemics., *Proceedings of the National Academy of Sciences of the United States of America* **114**, 4023 (2017).
- [13] M. E. Kretzschmar, G. Rozhnova, M. C. J. Bootsma, M. van Boven, J. H. H. M. van de Wijgert, and M. J. M. Bonten, Impact of delays on effectiveness of contact tracing strategies for covid-19: a modelling study., *The Lancet Public Health* **5**, e452 (2020).

- [14] K. O. Kwok, A. Tang, V. W. Wei, W. H. Park, E. K. Yeoh, and S. Riley, Epidemic models of contact tracing: Systematic review of transmission studies of severe acute respiratory syndrome and middle east respiratory syndrome., *Computational and Structural Biotechnology Journal* **17**, 186 (2019).
- [15] H. Kang, M. Sun, Y. Yu, X. Fu, and B. Bao, Spreading dynamics of an seir model with delay on scale-free networks., *IEEE Transactions on Network Science and Engineering, Network Science and Engineering, IEEE Transactions on, IEEE Trans. Netw. Sci. Eng* **7**, 489 (2020).
- [16] R. Pastor-Satorras and A. Vespignani, Epidemic dynamics and endemic states in complex networks., *Physical Review E (Statistical, Nonlinear, and Soft Matter Physics)* **63**, 066117/1 (2001).
- [17] L. Wang and G.-Z. Dai, Global stability of virus spreading in complex heterogeneous networks., *SIAM Journal on Applied Mathematics* **68**, 1495 (2008).
- [18] W. Kermak and A. McKendrick, Contributions to the mathematical-theory of epidemics .1. (reprinted from proceedings of the royal society, vol 115a, pg 700-721, 1927)., *Bulletin of Mathematical Biology* **53**, 33 (1991).
- [19] M. Martcheva, *Introduction to mathematical epidemiology.*, Texts in applied mathematics: v. 61 (New York : Springer, [2015], 2015).
- [20] D. W. Berger, K. F. Herkenhoff, and S. Mongey, An seir infectious disease model with testing and conditional quarantine., *NBER Working Papers* , 1 (2020).
- [21] Z. Kiss Istvan, M. Green Darren, and R. Kao Rowland, Disease contact tracing in random and clustered networks., *Proceedings: Biological Sciences* **272**, 1407 (2005).
- [22] L. Danon, A. P. Ford, T. House, C. P. Jewell, M. J. Keeling, G. O. Roberts, J. V. Ross, and M. C. Vernon, Networks and the epidemiology of infectious disease., *Interdisciplinary Perspectives on Infectious Diseases* , 1 (2011).
- [23] A. Aleta, D. Martín-Corral, A. P. Y. Piontti, M. Ajelli, M. Litvinova, M. Chinazzi, N. E. Dean, M. E. Halloran, J. Longini, Ira M, S. Merler, A. Pentland, A. Vespignani, E. Moro, and Y. Moreno, Modeling the impact of social distancing, testing, contact tracing and household quarantine on second-wave scenarios of the covid-19 epidemic., *MedRxiv : the preprint server for health sciences* (2020).
- [24] N. R. Initiative, *When to Test* (2020 (accessed December 15, 2020)).

- [25] Z. Feng and H. R. Thieme, Recurrent outbreaks of childhood diseases revisited: the impact of isolation., *Mathematical biosciences* **128**, 93 (1995).
- [26] J. Zhang and Z. Ma, Global dynamics of an seir epidemic model with saturating contact rate., *Mathematical Biosciences* **185**, 15 (2003).
- [27] D. Franco, H. Logemann, and J. Perán, Global stability of an age-structured population model., *Systems & Control Letters* **65**, 30 (2014).
- [28] L. J. S. Allen, S. R. Jang, and L.-I. Roeger, Predicting population extinction or disease outbreaks with stochastic models., *Letters in Biomathematics* **4**, 1 (2017).
- [29] C. Dwyer, *Coronavirus Has Infected A 5th Of New York City, Testing Suggests* (2020 (accessed December 15, 2020)).
- [30] G. G. Katul, A. Mrad, S. Bonetti, G. Manoli, and A. J. Parolari, Global convergence of covid-19 basic reproduction number and estimation from early-time sir dynamics., *PLoS ONE* **15**, 1 (2020).
- [31] K. Nagarajan, M. Muniyandi, B. Palani, and S. Sellappan, Social network analysis methods for exploring sars-cov-2 contact tracing data., *BMC medical research methodology* **20**, 233 (2020).
- [32] O. M. Tessa, Mathematical model for control of measles by vaccination, in *Proceedings of Mali Symposium on Applied Sciences*, Vol. 2006 (2006) pp. 31–36.
- [33] W. J. Edmunds, N. J. Gay, M. Kretzschmar, R. Pebody, and H. Wachmann, The pre-vaccination epidemiology of measles, mumps and rubella in europe: implications for modelling studies, *Epidemiology & Infection* **125**, 635 (2000).
- [34] L. F. White, J. Wallinga, L. Finelli, C. Reed, S. Riley, M. Lipsitch, and M. Pagano, Estimation of the reproductive number and the serial interval in early phase of the 2009 influenza a/h1n1 pandemic in the usa, *Influenza and other respiratory viruses* **3**, 267 (2009).
- [35] N. C. Grassly, C. Fraser, J. Wenger, J. M. Deshpande, R. W. Sutter, D. L. Heymann, and R. B. Aylward, New strategies for the elimination of polio from india, *Science* **314**, 1150 (2006).
- [36] G. Chowell, C. Castillo-Chavez, P. W. Fenimore, C. M. Kribs-Zaleta, L. Arriola, and J. M. Hyman, Model parameters and outbreak control for sars, *Emerging infectious diseases* **10**, 1258 (2004).
- [37] E. M. Nishiura H, Brockmann SO, Extracting key information from historical data to quantify the transmission dynamics of smallpox, *Theoretical Biology* 5:20 (2008).

- [38] Q. Li, X. Guan, P. Wu, X. Wang, L. Zhou, Y. Tong, R. Ren, K. S. M. Leung, E. H. Y. Lau, J. Y. Wong, X. Xing, N. Xiang, Y. Wu, C. Li, Q. Chen, D. Li, T. Liu, J. Zhao, M. Liu, W. Tu, C. Chen, L. Jin, R. Yang, Q. Wang, S. Zhou, R. Wang, H. Liu, Y. Luo, Y. Liu, G. Shao, H. Li, Z. Tao, Y. Yang, Z. Deng, B. Liu, Z. Ma, Y. Zhang, G. Shi, T. T. Y. Lam, J. T. Wu, G. F. Gao, B. J. Cowling, B. Yang, G. M. Leung, and Z. Feng, Early transmission dynamics in wuhan, china, of novel coronavirus-infected pneumonia., *The New England journal of medicine* **382**, 1199 (2020).
- [39] K. Mizumoto and G. Chowell, Transmission potential of the novel coronavirus (covid-19) onboard the diamond princess cruises ship, 2020., *Infectious Disease Modelling* **5**, 264 (2020).
- [40] CDC, *Past Seasons Estimated Influenza Disease Burden* (2020 (accessed December 15, 2020)).
- [41] K. Mizumoto and G. Chowell, Transmission potential of the novel coronavirus (covid-19) onboard the diamond princess cruises ship, 2020, *Infectious Disease Modelling* (2020).
- [42] S. Zhang, M. Diao, W. Yu, L. Pei, Z. Lin, and D. Chen, Estimation of the reproductive number of novel coronavirus (covid-19) and the probable outbreak size on the diamond princess cruise ship: A data-driven analysis, *International journal of infectious diseases* **93**, 201 (2020).
- [43] M. Iannelli and F. Milner, *The basic approach to age-structured population dynamics.*, Lecture Notes on Mathematical Modelling in the Life Sciences. (Springer, Dordrecht, 2017).
- [44] Z. Feng, C. Castillo-Chavez, and A. F. Capurro, A model for tuberculosis with exogenous reinfection., *Theoretical Population Biology* **57**, 235 (2000).
- [45] N. Ihor, Simulations and predictions of covid-19 pandemic with the use of sir model., *Innovative Biosystems and Bioengineering* **4**, 110 (2020).
- [46] S. Syed Tahir Ali, M. Majad, M. Adeel Feroz, D. Muhammad, K. Muhammad Imran, F. Rahat, K. Muhammad Ammar, B. Muhammad, and I. Hafiz M.N., Predicting covid-19 spread in pakistan using the sir model., *Journal of Pure and Applied Microbiology* **14**, 1423 (2020).
- [47] B. Malavika, S. Marimuthu, M. Joy, A. Nadaraj, E. S. Asirvatham, and L. Jeyaseelan, Forecasting covid-19 epidemic in india and high incidence states using sir and logistic growth models., *Clinical Epidemiology and Global Health* (2020).
- [48] P. Erdős and A. Rényi, On random graphs. i., *Publicationes Mathematicae Debrecen* **6**, 290 (1959).
- [49] A.-L. Barabasi and R. Albert, Emergence of scaling in random networks., in *Planning Models* (An Elgar Reference Collection. Classics in Planning series, vol. 2. Cheltenham, U.K. and

Northampton, Mass.: Elgar, Unlisted, 2006) pp. 427 – 430.